Volume Conduction Effects on Connectivity Metrics: Application of Network Parameters to Characterize Alzheimer's Disease Continuum

Saúl J. Ruiz-Gómez, Carlos Gómez, *IEEE Senior Member*, Jesús Poza, *IEEE Senior Member*, Marcos Revilla-Vallejo, Víctor Gutiérrez-de-Pablo, Víctor Rodríguez-González, Aarón Maturana-Candelas, Roberto Hornero, *IEEE Senior Member*

***Abstract*— This study had two main objectives: (i) to study the effects of volume conduction on different connectivity metrics (Amplitude Envelope Correlation *AEC*, Phase Lag Index *PLI*, and Magnitude Squared Coherence *MSCOH*), comparing the coupling patterns at electrode- and sensor-level; and (ii) to characterize spontaneous EEG activity during different stages of Alzheimer's disease (AD) continuum by means of three complementary network parameters: node degree (*k*), characteristic path length (*L*), and clustering coefficient (*C*). Our results revealed that *PLI* and *AEC* are weakly influenced by volume conduction compared to *MSCOH*, but they are not immune to it. Furthermore, network parameters obtained from *PLI* showed that AD continuum is characterized by an increase in *L* and *C* in low frequency bands, suggesting lower integration and higher segregation as the disease progresses. These network changes reflect the abnormalities during AD continuum and are mainly due to neuronal alterations, because *PLI* is slightly affected by volume conduction effects.**

I. INTRODUCTION

The human brain can be conceptualized as a complex network in which billions of neurons interact. EEG allows measuring the brain electrical activity generated by synchronized cortical neurons in a non-invasive way with a high temporal resolution. However, time series that are recorded from nearby sensors are very likely to pick up activity from the same brain sources, which gives rise to spurious correlations between them. This is known as the problem of 'volume conduction' [1]. Many source localization methods have been developed to estimate the underlying source activity and overcome the volume conduction problem. Nevertheless, source inversion is an ill-posed problem and different methods use specific types of assumptions to restrict the results and provide a unique solution [2].

Dementia due to Alzheimer's disease (AD) is a progressive neurodegenerative disorder that is the most common cause of dementia. AD is usually preceded by a prodromal stage known as mild cognitive impairment (MCI), with a conversion rate to AD of approximately 15% per year, whereas healthy controls conversion rate is only 1%–2% per year [3]. Furthermore, depending on the affected brain regions and the symptoms, three different stages can be distinguished during AD evolution: mild AD (AD_{mil}), moderate AD (AD_{mod}), and severe AD (AD_{sev}).

EEG activity from MCI and AD patients is progressively modified as a consequence of the pathophysiological processes. Traditionally, EEG recordings in AD have been analyzed using local activation techniques in individual sensors (both spectral and non-lineal analyses) [4]. However, in order to study the AD brain as a complex network, the application of connectivity metrics and parameters derived from graph theory have focused great attention. In this regard, it is important to use a connectivity metric that minimizes the spurious correlations that can appear due to volume conduction.

Our main objectives were to evaluate how different connectivity metrics are affected by volume conduction and to analyze the ability of different network parameters to characterize the brain networks during the AD progression. Specifically, the following research questions were addressed: (i) which of the analyzed connectivity metrics shows the higher relationship between source-level and electrode-level results?; and (ii) are network parameters derived from these measures capable of reflecting brain alterations during AD continuum at electrode-level?

II. MATERIALS

A. Subjects

EEG resting-state activity was analyzed in 51 healthy controls (age 80.1 $\pm$ 7.1 years, mean $\pm$ standard deviation), 51 MCI subjects (age 85.5 $\pm$ 7.2 years), 51 mild AD patients (age 80.5 $\pm$ 6.9 years), 50 moderate AD patients (age 81.3 $\pm$ 8.0 years), and 50 severe AD patients (age 80.0 $\pm$ 7.8 years). Patients with MCI and dementia due to AD were diagnosed according to the criteria of the National Institute on Aging and Alzheimer's Association (NIA-AA).

This research was supported by 'Ministerio de Ciencia, Innovación y Universidades' and 'European Regional Development Fund' (FEDER) under project PGC2018-098214-A-I00, by 'European Commission' and 'FEDER' under projects 'Análisis y correlación entre el genoma completo y la actividad cerebral para la ayuda en el diagnóstico de la enfermedad de Alzheimer' and 'Análisis y correlación entre la epigenética y la actividad cerebral para evaluar el riesgo de migraña crónica y episódica en mujeres' ('Cooperation Programme Interreg V-A Spain-Portugal POCTEP 2014–2020'), and by 'CIBER de Bioingeniería, Biomateriales y Nanomedicina (CIBER-BBN)' through 'Instituto de Salud Carlos III' co-funded with FEDER funds. Saúl J. Ruiz-Gómez was in receipt of a predoctoral scholarship from the 'Junta de Castilla y León' and the 'European Social Fund'.

Saúl J. Ruiz-Gómez, Carlos Gómez, Jesús Poza, Marcos Revilla-Vallejo, Víctor Gutiérrez-de-Pablo, Víctor Rodríguez-González, Aarón Maturana-Candelas, and Roberto Hornero are with the Biomedical Engineering Group, University of Valladolid, Valladolid, Spain, and with Centro de Investigación Biomédica en Red en Bioingeniería, Biomateriales y Nanomedicina, (CIBER-BBN), Spain. (corresponding author's e-mail: saul.ruiz@gib.tel.uva.es).

The control group was composed of elderly subjects with no history of neurological or psychiatric disorders.

Participants and caregivers were informed about the research background and the study protocol. All of them gave their written informed consent to be included in the study. The Ethical Committee of the Porto University (Porto, Portugal) approved the study according to the Code of Ethics of the World Medical Association (Declaration of Helsinki).

B. Electroencephalographic recordings

Five minutes of resting-state EEG activity was recorded with a 19-channel system at a sampling frequency of 500 Hz (Nihon Kohden Neurofax JE-921A). Electrodes were placed following the 10-20 International System at: Fp1, Fp2, Fz, F3, F4, F7, F8, Cz, C3, C4, T3, T4, T5, T6, Pz, P3, P4, O1, and O2. Subjects were asked to remain with their eyes closed, still and awake during EEG acquisition.

Then, recordings were preprocessed in three steps [5]: (i) independent component analysis to remove components with artifacts; (ii) FIR filtering using a Hamming window filter to limit the spectral content to the frequency band of [1 70] Hz; and (iii) visual selection of artifact-free epochs of 5s.

III. METHODS

A. Source reconstruction: sLORETA

Time series at source level were obtained using standardized low resolution brain electromagnetic tomography (sLORETA), available in Brainstorm (http://neuroimage.usc.edu/brainstorm) [6]. Since there is no unique solution to the inverse problem, sLORETA is based on a model of lineal distributed source. It provides a solution assuming that nearby neurons are synchronized, maximizing the correlation between neighboring sources [7]. In addition, sLORETA applies physiological restrictions on the estimated sources to reduce the errors. The high dimensionality of the source-level signals was limited using the Desikan-Killiany atlas to project the signals in 68 Regions of Interest (ROIs). Technical details of the method are described in [7].

B. Connectivity metrics

In order to compare the connectivity results at electrode and source-level, three complementary coupling metrics were analyzed: Amplitude Envelope Correlation (AEC), Phase Lag Index (PLI), and Magnitude Squared Coherency ($MSCOH$).

AEC is an estimation of the correlation between the amplitudes of two time series. Firstly, time series were orthogonalized in order to remove spatial leakage effects [8]. Then, AEC is obtained by computing the Pearson correlation between the log transformed power envelopes using the Hilbert transform [9].

PLI between two time-series quantifies the asymmetry in the distribution of phase differences [1]:

$$PLI = |\langle sign \sin(\Delta\phi)\rangle|, \tag{1}$$

where $\langle\cdot\rangle$ indicates the expectation operator and $\Delta\phi$ is the phase difference or relative phase.

$MSCOH$ measures the similarities in the frequency content of two signals, combining both amplitude and phase information. It is defined as [10]:

$$MSCOH_{X,Y}(f) = \frac{|S_{XY}|^2}{P_X P_Y}, \tag{2}$$

where S_{XY} is the cross-spectrum of signals X and Y, and P_X and P_Y are the power spectral density of X and Y, respectively.

The result of computing each measure for all pair-wise combinations was a 19 x 19 matrix for the electrode-level (corresponding to 19 electrodes) and a 68 x 68 matrix for the source-level (68 ROIs).

C. Network parameters

Network parameters derived form graph theory summarize one or several aspects of global and local brain connectivity. In this study, we analyzed three complementary metrics: mean node degree (k), characteristic path length (L), and clustering coefficient (C).

k is a basic centrality metric that represents the total 'wiring cost' of the whole network. It is defined as the node-average of the sum of all neighboring link weights [11]:

$$k = \frac{1}{N} k_i = \frac{1}{N} \sum_{j \in N} a_{ij}, \tag{3}$$

where a_{ij} is the connectivity value between nodes i and j and N is the total number of nodes.

L is the most commonly used measure of integration and is defined as the average shortest path length between all pairs of nodes in the network [11]:

$$L = \frac{1}{N} \sum_{i \in N} \frac{\sum_{j \in N, j \neq i} d_{ij}}{N-1}, \tag{4}$$

where d_{ij} is the shortest path length (distance) between nodes i and j.

C is a segregation metric and represents the fraction of the node neighbors that are also neighbors of each other. It reflects, on average, the prevalence of clustered connectivity around individual nodes [11]. Mathematically, it is defined as [11]:

$$C = \frac{1}{N} \sum_{i \in N} \frac{2t_i}{k_i(k_i - 1)}, \tag{5}$$

where t_i is the geometric mean of triangles of each node.

D. Statistical analysis

In order to study how the connectivity metrics are affected by volume conduction, the correlation between source and electrode connectivity results was performed using the Pearson correlation coefficient. Then, their ability to obtain statistical differences between all groups were evaluated with the Kuskal-Wallis test, while differences between pairwise groups were evaluated using the Mann-Whitney U-test.

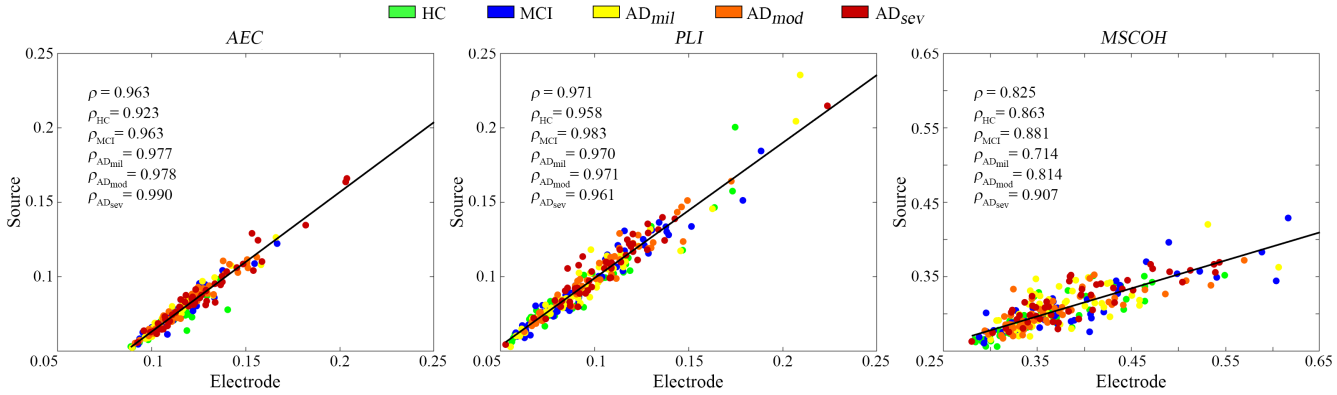

Fig. 1. Grand-average AEC, PLI, and $MSCOH$ scatterplots of electrode and source results. The correlation strength is reported as Pearson ρ values.

IV. RESULTS

A. Connectivity metrics

The scatterplots for the averaged connectivity metrics in the global band (1-70 Hz) are displayed in Fig. 1. The Pearson correlation values between electrode and source results were high for the three analyzed metrics. Specifically, PLI showed the highest correlation values taking into account all groups together ($\rho = 0.971$), compared to AEC ($\rho = 0.963$) and COH ($\rho = 0.825$). Comparing the different groups under analysis, PLI and AEC showed similar correlation values, higher than the ones obtained using $MSCOH$. Furthermore, the ability of these metrics to mitigate volume conduction effects was evaluated comparing the electrode- and source-level results obtained for each subject. In this case, AEC showed similar but slightly higher values at the electrode level compared to source level, exhibiting an offset independent of the coupling level. $MSCOH$ presented a similar trend but its offset is higher as the real-source connectivity increases. Finally, PLI displayed similar values without any offset, showing the highest correlation among the analyzed metrics. For these reasons, the subsequent network analysis was only performed using PLI networks.

B. Network parameters

Fig. 2 displays k, L, and C values for each frequency band using the metric less affected by volume conduction effects (PLI) as the connectivity measure at the electrode-level. Similar results were obtained for source-level. Since results are frequency-dependent, these parameters were computed for the six conventional EEG-frequency bands: delta (1-4 Hz), theta (4-8 Hz), alpha (8-13 Hz), beta-1 (13-19 Hz), beta-2 (19-30 Hz), and gamma (30-70 Hz).

Our results using k revealed an increasing trend of global connectivity at the theta band, and a global decrease at alpha band as the disease progresses. Taking into account differences between pair-wise groups, HC subjects showed statistically significant lower k values compared with the other groups at theta band. On the other hand, the behavior was the opposite at the alpha band, where AD$_{sev}$ patients obtained statistically significant lower k values than the other groups. In addition, our L results showed significant

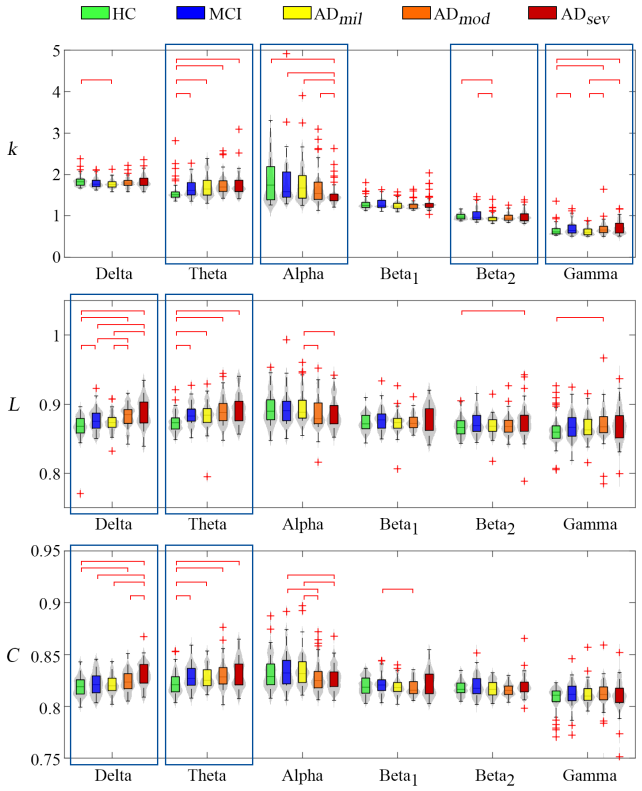

Fig. 2. Averaged k, L, and C distribution plots computed from PLI connectivity matrices in each conventional EEG frequency-band for each group at the electrode-level. Statistically significant between-group differences are marked with blue rectangles ($p < 0.05$, Kruskal-Wallis test) and pairwise differences are marked with red brackets ($p < 0.05$, Mann-Whitney U-test).

higher values as dementia severity increases at delta and theta frequency bands. In the delta band, most of these differences between groups were statistically significant, whereas in the theta band only between HC subjects and the other groups. However, results obtained with L in the alpha band showed a slightly decrease as AD severity increases, being only significant for AD$_{mil}$ vs. AD$_{mod}$ and AD$_{sev}$ comparisons. Finally, C followed a very similar trend compared to L, with significant increments at delta and theta, and decrements at alpha as AD progresses.

V. DISCUSSION

In the present study, we analyzed the behavior of three different connectivity metrics (AEC, PLI, and $MSCOH$) to overcome the spurious effects introduced by EEG volume conduction comparing the obtained values at electrode and source levels. In addition, we evaluated the ability of three complementary network parameters to summarize the properties of the obtained networks during AD continuum.

In order to answer the first research question, we compared the correlation between the averaged connectivity results at the electrode and source level. Only Lai *et al.* [12] have previously employed a similar methodology to compare average connectivity values between source and scalp level. Their results showed that AEC and PLI had a very similar performance ($\rho = 0.890$ and $\rho = 0.878$, respectively). Their dataset is only comprised by 109 control subjects [12]. In our study, we used a larger database comprised by HC subjects, MCI patients, and mild, moderate, and severe AD patients. This has allowed us to have a higher statistical power and to evaluate the connectivity metrics behavior taking into account different brain conditions produced by the neurodegenerative processes, such as decreased hippocampal volume or gray matter density loss [13]. These structural brain changes yield to produce different volume conduction effects for each group under study, as reflected by the variation in the correlation coefficient between different groups (see Fig.1). This analysis has allowed us to determine that PLI has the best performance detecting real coupling when comparing source and electrode levels. These results are in line with the ones obtained in our previous work using synthetic signals [5].

Furthermore, our database has been analyzed using three different graph theory parameters from the PLI connectivity networks. Network parameters in low frequency bands (delta and theta) indicated that networks are characterized by higher average connectivity as the disease progresses (revealed by an increase in the average node degree), lower integration (increase in the characteristic path length), and higher segregation (increase in clustering coefficient). These findings are in line with studies that reported decreased integration and increased segregation observed in AD patients compared with HC subjects [14], [15]. One possible clinical interpretation for the increased C reflects a compensatory mechanism that is triggered by the dysfunctional integration in AD brain networks [15]. In this regard, a longitudinal study also reported a higher L and increased C during AD progression [16].

This study has two main limitations. Firstly, network parameters were computed in the classical EEG frequency bands to characterize the AD continuum. This approach could lead to obtain contradictory results when comparing frequency bands. Thus, multiplex network approaches may be useful to summarize all information in only one value, easier to interpret [17]. Secondly, despite we had the AD continuum divided into four severity groups, it would be useful to perform a longitudinal study focused on MCI subjects. This could allow us to study the changes of the subjects that remain stable and those that progress to AD.

VI. CONCLUSIONS

In conclusion, the present study confirms that functional connectivity metrics are not immune to volume conduction, but PLI is the least affected when electrode and source results are compared. Different network parameters (k, L, and C) computed from PLI networks have proven their usefulness to summarize different network properties and reflect the brain changes caused in the different stages of AD continuum, from MCI to AD_{sev}. These results suggest that, as the disease severity increases, network topologies tend to be less integrated and more segregated, reducing their global performance and enhancing their local performance. These network changes seem to be due to alterations in neuronal activity in dementia, since they are computed using PLI, the metric less affected by volume conduction effects.

REFERENCES

[1] C. J. Stam *et al.*, "Phase lag index: Assessment of functional connectivity from multi channel EEG and MEG with diminished bias from common sources," *Human Brain Mapping*, vol. 28, pp. 1178–1193, 2007.

[2] S. Sanei and J. A. Chambers, *EEG Signal Processing*, 2013.

[3] Alzheimer's Association, "2017 Alzheimer's Disease Facts and Figures," *Alzheimers Dement*, vol. 13, pp. 325–373, 2017.

[4] J. Jeong, "EEG dynamics in patients with Alzheimer's disease," *Clinical Neurophysiology*, vol. 115, no. 7, pp. 1490–1505, jul 2004.

[5] S. J. Ruiz-Gómez *et al.*, "Computational modeling of the effects of EEG volume conduction on functional connectivity metrics. Application to Alzheimer's disease continuum," *Journal of Neural Engineering*, vol. 16, p. 066019, 2019.

[6] F. Tadel *et al.*, "Brainstorm: A user-friendly application for MEG/EEG analysis," *Computational Intelligence and Neuroscience*, vol. 879716, pp. 1–13, 2011.

[7] R. D. Pascual-Marqui, "Standardized low-resolution brain electromagnetic tomography (sLORETA): Technical details," *Methods and Findings in Experimental and Clinical Pharmacology*, vol. 24 Suppl D, pp. 5–12, 2002.

[8] G. O'Neill *et al.*, "Dynamics of large-scale electrophysiological networks: A technical review," *NeuroImage*, vol. 180, pp. 559–576, 2018.

[9] M. J. Brookes *et al.*, "Measuring temporal, spectral and spatial changes in electrophysiological brain network connectivity," *NeuroImage*, vol. 91, pp. 282–299, 2014.

[10] B. J. Roach and D. H. Mathalon, "Event-related EEG time-frequency analysis: An overview of measures and an analysis of early gamma band phase locking in schizophrenia," *Schizophrenia Bulletin*, vol. 34, no. 5, pp. 907–926, 2008.

[11] M. Rubinov and O. Sporns, "Complex network measures of brain connectivity: Uses and interpretations," *NeuroImage*, vol. 52, pp. 1059–1069, 2010.

[12] M. Lai *et al.*, "A comparison between scalp- and source-reconstructed EEG networks," *Scientific Reports*, vol. 8, p. 12269, 2018.

[13] G. B. Karas *et al.*, "Global and local gray matter loss in mild cognitive impairment and Alzheimer's disease," *NeuroImage*, vol. 23, pp. 708–716, 2004.

[14] C. J. Stam *et al.*, "Graph theoretical analysis of magnetoencephalographic functional connectivity in Alzheimer's disease," *Brain*, vol. 132, pp. 213–224, 2009.

[15] S. Afshari and M. Jalili, "Directed Functional Networks in Alzheimer's Disease: Disruption of Global and Local Connectivity Measures," *IEEE Journal of Biomedical and Health Informatics*, vol. 21, pp. 949–955, 2017.

[16] F. C. Morabito *et al.*, "A longitudinal EEG study of Alzheimer's disease progression based on a complex network approach," *International Journal of Neural Systems*, vol. 25, p. 1550005, 2015.

[17] N. Amoroso *et al.*, "Multiplex networks for early diagnosis of Alzheimer's disease," *Frontiers in Aging Neuroscience*, vol. 14, no. 10, pp. 1–15, 2018.